Shallow acceptor impurity states in V-shaped GaAs-$Ga_{1-x}Al_xAs$ quantum wires

2000 J. Phys.: Condens. Matter 12 3019

(http://iopscience.iop.org/0953-8984/12/13/312)

J. Phys.: Condens. Matter **12** (2000) 3019–3027. Printed in the UK PII: S0953-8984(00)08159-5

Shallow acceptor impurity states in V-shaped GaAs–$Ga_{1-x}Al_xAs$ quantum wires

Zhen-Yan Deng†, Tatsuki Ohji† and Xiaoshuang Chen‡

† Synergy Ceramics Laboratory, FCRA & NIRIN, Joint Research Consortium of Synergy Ceramics, Cooperative Research Center for Advanced Technology, Shidami Human Science Park, 2268-1, Simo-Shidami, Moriyama-ku, Nagoya 463-8687, Japan
‡ Department of Physics, School of Science, University of Tokyo, 7-3-1 Hongo, Bunkyo-ku, Tokyo 113, Japan

E-mail: zydeng@nirin.go.jp

Received 27 September 1999

Abstract. The shallow acceptor impurity states in V-shaped GaAs–$Ga_{1-x}Al_xAs$ quantum wires (V-QWRs) are investigated by a coordinate transformation method. An asymmetrical distribution of impurity binding energy along the direction normal to the V-shaped boundaries is found. The impurity position corresponding to the maximum binding energy deviates from the centre of V-QWRs. The variations in impurity binding energy with the dimension and curvatures of V-QWRs are discussed.

1. Introduction

One-dimensional V-shaped and T-shaped semiconductor quantum wires have received considerable attention in the past few years, due to the rapid development of material growth techniques [1, 2]. Because the quantum confinement in one-dimensional systems increases the importance of excitonic effects and enhances the density of states at specific energies [3–5], quantum wire structures have wide potential applications in microelectronics and future laser technology [6]. The experimental works on these quantum wire structures are very wide and intensive, including the growth dynamics [7–9], photoluminescence (PL) and photoluminescence excitation (PLE) spectra [10, 11], exciton recombination dynamics [12, 13] and electric transport [14], etc. Because of the special cross-section shapes of V-shaped and T-shaped quantum wires, it is not easy to obtain a simple and intuitive wavefunction for their electronic states. In order to explain and explore the physical mechanisms in these quantum wire structures, a number of theoretical methods were proposed [5, 10, 15–19].

The coordinate transformation method is an effective method to deal with the subband structures in low-dimensional systems with nonplanar interfaces [19–21]. In this method, the nonplanar interfaces become planar ones after a coordinate transformation so that the boundary conditions of electronic wavefunctions can be satisfied exactly on the interfaces. In a previous paper [22], the subband structures and exciton transitions in V-QWRs were investigated by the coordinate transformation method with a variational procedure, and the theoretical exciton peaks are in good agreement with the recent experimental PLE spectra [10]. In this paper, the acceptor impurity states in V-QWRs are studied, as the impurity states are an important factor to affect the electric-transportation and optical properties in semiconductor structures.

0953-8984/00/133019+09$30.00

In section 2, a theoretical framework is outlined. Numerical results and discussion are presented in section 3.

2. Theory

Figure 1 is a schematic representation of V-QWRs, where GaAs is the well material and $Ga_{1-x}Al_xAs$ is the barrier material. Electron and hole are confined in the x–y plane and free in the z direction. When an acceptor impurity is placed inside the V-QWRs, in the effective-mass approximation, the Hamiltonian for impurity states can be written

$$H(\vec{r}) = V_{ion}(\vec{r}) + \begin{cases} \vec{P}^2/(2m_1) & -d + f_2(x) < y < d + f_1(x) \\ \vec{P}^2/(2m_2) + V_0 & \text{elsewhere} \end{cases} \tag{1}$$

and

$$V_{ion}(\vec{r}) = -e^2/(\varepsilon|\vec{r} - \vec{r}_0|) \tag{2}$$

where $\vec{r}$ and $\vec{P}$ are the hole coordinate and momentum, respectively; $\vec{r}_0$ is the impurity position; m_1 and m_2 are the hole effective mass in the well material and barrier material, respectively; ε is the dielectric constant, and the difference in dielectric constant between the well material and barrier material is neglected; V_0 is the hole-confining potential, which is equal to the valence-band discontinuity between the barrier material and well material; $d + f_1(x)$ and $-d + f_2(x)$ represent the upper and bottom boundaries of the V-QWR, respectively. Since the alloy composition we considered is direct ($x < 0.45$), both the effective mass m_2 and the valence-band offset V_0 can be determined by the following $\vec{k} = 0$ values in $Ga_{1-x}Al_xAs$ [23, 24]

$$\begin{aligned} m_1 &= 0.51m_0 \\ m_2 &= (0.51 + 0.25x)m_0 \\ V_0 &= 0.35\Delta E_g^{\Gamma}(x) \\ \varepsilon &= 12.6\varepsilon_0 \end{aligned} \tag{3}$$

where the mixing of heavy-hole and light-hole states is neglected; m_0 is the free-electron mass and ε_0 is the vacuum static dielectric constant; $\Delta E_g^{\Gamma}(x)$ is the difference between the $Ga_{1-x}Al_xAs$ and GaAs band gaps at the Γ point, which is given by [24]

$$\Delta E_g^{\Gamma}(x) = 1.247x \text{ eV}. \tag{4}$$

The following coordinate transformation

$$\begin{aligned} x' &= x \\ y' &= \frac{d}{2d + [f_1(x) - f_2(x)]}[2y - [f_1(x) + f_2(x)]] \\ z' &= z \end{aligned} \tag{5}$$

transforms the V-shaped boundaries into planar ones, and the wavefunctions could satisfy the boundary conditions exactly on the interfaces. After the coordinate transformation, the confining potential becomes

$$V(\vec{r}) = \begin{cases} 0 & |y'| < d \\ V_0 & \text{elsewhere.} \end{cases} \tag{6}$$

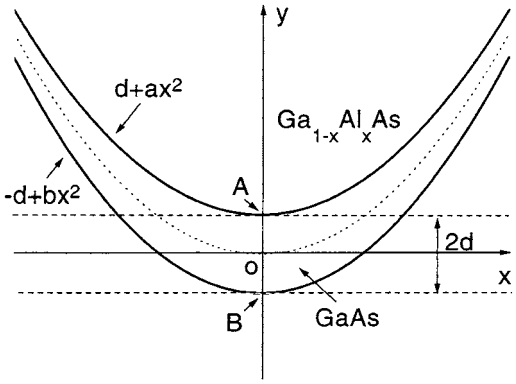

Figure 1. A schematic representation of V-QWRs, where $d + ax^2$ and $-d + bx^2$ are the upper and bottom boundaries, respectively. The dotted line represents the middle line $y = (a + b)x^2/2$ of V-QWRs, and the dashed lines represent the new boundaries after the coordinate transformation.

The V-shaped boundaries become a confining potential along the x direction, which is included in the new Hamiltonian, so that the electron and hole feel the confinement in two directions like that in the traditional quantum wires with rectangular and circular cross sections

$$\frac{\int \psi^*(\vec{r})H(\vec{r})\psi(\vec{r})\,\mathrm{d}V}{\int \psi^*(\vec{r})\psi(\vec{r})\,\mathrm{d}V} = \frac{\int \psi^*(\vec{r'})|J(\vec{r'})|H(\vec{r'})\psi(\vec{r'})\,\mathrm{d}V'}{\int \psi^*(\vec{r'})|J(\vec{r'})|\psi(\vec{r'})\,\mathrm{d}V'} \tag{7}$$

where $J(\vec{r'})$ is the Jacobian determinant.

The impurity state behaviour in traditional quantum wires has been studied by many researchers [25–33], and a number of interesting and valuable results were obtained. The traditional method to calculate the impurity binding energy in quantum wires is the variational method, due to no exact solutions to the impurity states in quantum wires. The following trial wavefunction in the new coordinate space is adopted for the ground impurity state in V-QWRs

$$\psi(\vec{r'}) = \psi_0(\vec{r'})\exp(-\beta|\vec{r'} - \vec{r'_0}|) \tag{8}$$

and the acceptor impurity binding energy is defined as follows [34]

$$E_b = E_0 - \min_{\beta}\langle\psi(\vec{r'})|J(\vec{r'})H(\vec{r'})|\psi(\vec{r'})\rangle/\langle\psi(\vec{r'})|J(\vec{r'})|\psi(\vec{r'})\rangle \tag{9}$$

where β is a variational parameter and $\vec{r'}_0$ is the impurity position after the coordinate transformation; $\psi_0(\vec{r'})$ and E_0 are the ground hole wavefunction and ground hole level in V-QWRs, respectively, which can be obtained by the procedures developed in our previous paper [22]. In the previous paper [22], the hole subband wavefunctions are the combination of complete quantum well eigenstates in the y direction and the complete harmonic oscillator eigenstates in the x direction (due to the harmonic-like potential in the x direction after coordinate transformation). The above trial wavefunction satisfies the boundary conditions on the interfaces.

3. Results and discussion

Our previous results [22] show that a parabola is a good function to fit the upper and bottom boundaries of V-QWRs, because the calculated exciton peaks are in good agreement with the experimental PLE spectra. Technically, the functions used to fit V-shaped boundaries can be

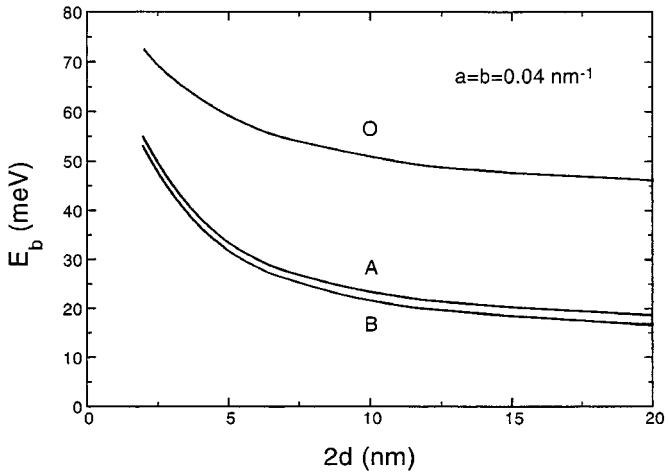

Figure 2. Variations in impurity binding energy with the dimension of V-QWRs for three different impurity positions, where the Al composition in barrier material is $x = 0.4$ and the curvatures of V-shaped boundaries are fixed.

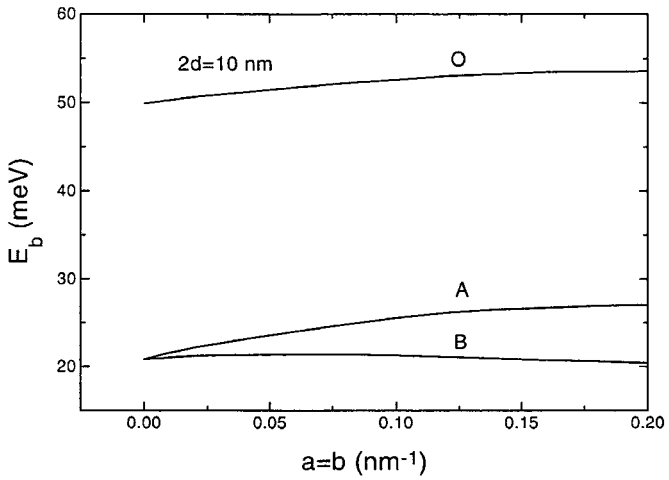

Figure 3. Variations in impurity binding energy with the curvatures of V-shaped boundaries for three different impurity positions, where the Al composition in barrier material is $x = 0.4$ and the dimension of V-QWRs is fixed.

arbitrary, and there is no difficulty for us to finish the calculations for more complicated boundary functions. For a model analysis, two parabolas, that is, $f_1(x) = ax^2$ and $f_2(x) = bx^2$, are selected to represent the upper and bottom boundaries of V-QWRs, as shown in figure 1.

Figures 2 and 3 show the variations in acceptor impurity binding energy with the dimension and curvatures of V-QWRs for three different impurity positions, respectively, where O is the centre of V-QWRs and A and B are the cross points of the upper and bottom V-shaped boundaries with the y-axis (see figure 1). Here, the upper and bottom boundaries with the same curvatures ($a = b$) are considered, as in most cases, the two boundaries of V-QWRs do not cross each other in the experiments [1, 8–10]. The variation range of the dimension and

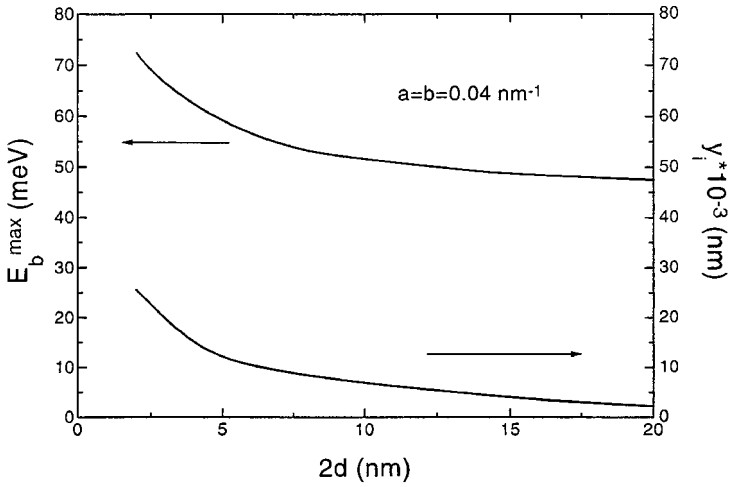

Figure 4. Dependence of maximum impurity binding energy and its corresponding impurity position ($x_i = 0$) on the dimension of V-QWRs, where the Al composition in barrier material is $x = 0.4$ and the curvatures of V-shaped boundaries are fixed.

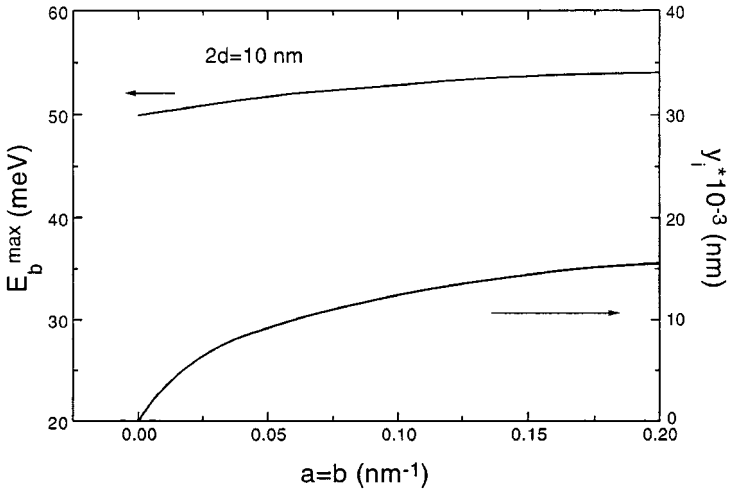

Figure 5. Dependence of maximum impurity binding energy and its corresponding impurity position ($x_i = 0$) on the curvatures of V-shaped boundaries, where the Al composition in barrier material is $x = 0.4$ and the dimension of V-QWRs is fixed.

curvatures of V-QWRs we adopted in figures 2 and 3 has been realized in the experiments [8–10]. From figure 2, it can be seen that the impurity binding energy increases with the decrease in the dimension of V-QWRs, due to the enhancement of the confining potential in V-QWRs. However, the peak impurity binding energy, which usually appears in the *binding energy versus dimension* curves in traditional quantum wires with finite confining potential [26, 31] due to the leakage of the wavefunction from well material, does not appear in our results. This may be due to the heavier hole effective mass we adopted in this study and the resultant smaller effective hole Bohr radius ($a_0^* = \hbar^2\varepsilon/(m_h e^2) = 13.07$ Å in the GaAs well material), which causes the peak dimension of V-QWR to be too small and beyond the

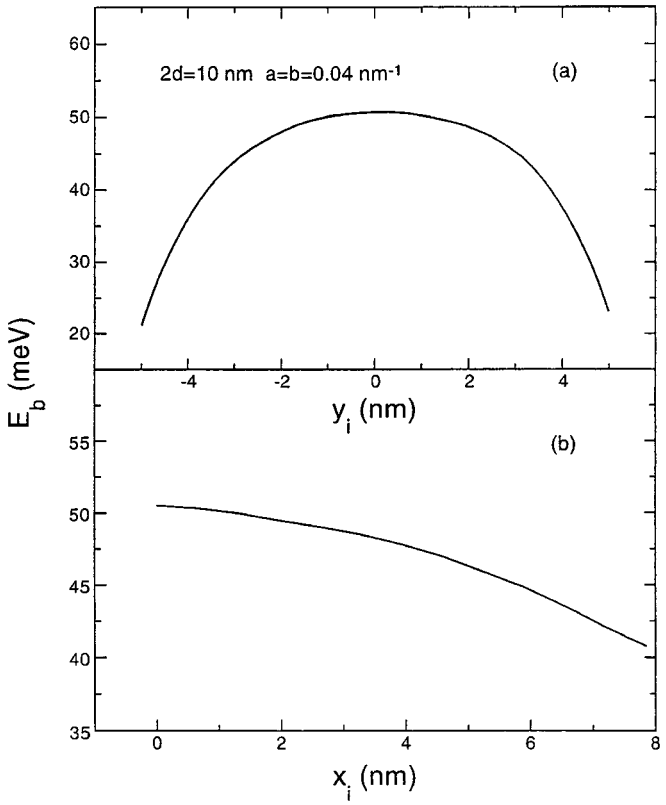

Figure 6. Variations in impurity binding energy with the impurity position (a) along the y-axis ($x_i = 0$) and (b) along the middle line (the dotted line shown in figure 1) of a V-QWR, where the Al composition in the barrier material is $x = 0.4$, and the dimension and curvatures are fixed.

dimension range that we considered. By the way, if the dimension of V-QWRs is too small, the effective-mass approximation used here may not be applicable. In figure 2, it can also be seen that the impurity binding energy at the centre is larger than that at two boundary points, and the impurity binding energy at upper boundary point A is larger than that at bottom boundary point B. This implies that there is an asymmetrical distribution of impurity binding energy along the direction normal to the boundaries, due to the asymmetrical confining potential in the y direction, which is different from the impurity state behaviour in traditional quantum wires [25, 26, 31]. The asymmetrical confining potential in the y direction can be seen from the geometry of V-QWRs. It is apparent that most of the wavefunctions are pushed towards the convex side in the well, due to the shape of the barrier boundaries. This means that the wavefunctions are asymmetrical in the y direction, and the centre of gravity of the wavefunctions moves towards the convex side in the well; so the impurity binding energy at two boundary cross points is different. When the curvatures of V-shaped boundaries increase, the confining potential in the x direction increases, which causes the impurity binding energy to increase, as shown in figure 3. At the same time, the increase in the curvatures of V-shaped boundaries increases the asymmetry of confining potential in the y direction, and the difference in binding energy between the upper and bottom boundary points increases. The decrease in binding energy at bottom boundary point B for the higher curvatures of V-shaped boundaries in figure 3 is related to the serious leakage of the wavefunction in the well material.

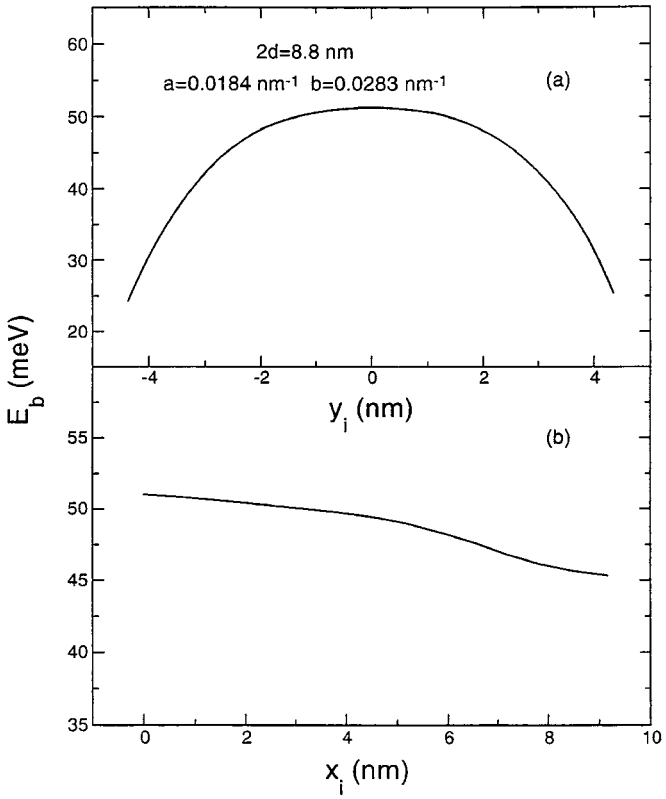

Figure 7. Variations in impurity binding energy with the impurity position (a) along the y-axis ($x_i = 0$) and (b) along the middle line (the dotted line shown in figure 1) of a real V-QWR in [10], where the Al composition in the barrier material is $x = 0.3$. The dimension $2d$ and the curvatures a, b of V-shaped boundaries were obtained by fitting the boundaries of real V-QWR.

Because of the asymmetrical confining potential in the y direction, it is found that the impurity position corresponding to maximum binding energy deviates from the centre of V-QWRs. The dependence of maximum impurity binding energy and its corresponding impurity position on the dimension and curvatures of V-QWRs are shown in figures 4 and 5. Figures 4 and 5 show that the variations in maximum binding energy with the dimension and curvatures of V-QWRs are similar to those in figures 2 and 3. The deviation of peak impurity position from the centre decreases with the increase in the dimension and increases with the increase in the curvatures of V-QWRs, depending on the deviation of the centre of gravity of the impurity state wavefunctions.

In order to understand clearly the asymmetrical confining potential in the y-direction, figures 6 and 7 show the dependence of impurity binding energy on the impurity position along the y-axis and the middle line between two V-shaped boundaries. The quantum wire structure in figure 7 is a real V-QWR in [10], and its width and curvatures were obtained by fitting the real V-shaped boundaries measured from a TEM micrograph [10, 22]. The asymmetrical distribution of impurity binding energy along the y-direction can be clearly seen in figures 6(a) and 7(a), and the centre of gravity of the binding energy distribution in the y-direction moves towards the convex side of V-QWRs. The distribution of impurity binding energy along the middle line of the V-QWR is symmetrical, due to the symmetrical boundaries

and its resultant symmetrical potential in the x-direction. It is apparent that the impurity binding energy along the middle line decreases as the impurity position is further away from the centre of V-QWRs, as shown in figures 6(b) and 7(b). This behaviour is similar to the variations in impurity binding energy with the impurity position within the cross section of traditional quantum wires [25, 26, 29, 31]. Moreover, figures 6 and 7 show that the impurity state behaviour has no qualitative difference for the V-QWRs, in which the upper and bottom boundaries have or do not have the same curvature. If other different types of function, which more exactly describe the V-shaped boundaries, are used to represent V-shaped boundaries, it is believed that the above qualitative results have no change, though there are some small quantitative changes in impurity binding energy in V-QWRs.

In summary, the shallow acceptor impurity states in V-QWRs are investigated by a coordinate transformation method. It is found that the impurity state behaviour in V-QWRs in a sense is similar to that in traditional quantum wires. However, there is an asymmetrical distribution of impurity binding energy along the direction normal to the V-shaped boundaries, due to the asymmetrical confining potential. The impurity position corresponding to the maximum binding energy deviates from the centre of V-QWRs.

Acknowledgments

The authors are grateful to Professor K J Chang and Professor Steven G Louie at Berkeley for their helpful suggestions. This work was supported by NEDO and JSPS in Japan.

References

[1] Kapon E, Hwang D M and Bhat R 1989 *Phys. Rev. Lett.* **63** 430
[2] Akiyama H 1998 *J. Phys.: Condens. Matter* **10** 3095 (and references therein)
[3] Ogawa T and Takagahara T 1991 *Phys. Rev.* B **44** 8138
[4] Glutsch S and Bechstedt F 1993 *Phys. Rev.* B **47** 4315
[5] Rossi F and Molinari E 1996 *Phys. Rev. Lett.* **76** 3642
[6] Tiwari S, Pettit G D, Milkove K R, Legoues F, Davis R J and Woodall J M 1994 *Appl. Phys. Lett.* **64** 3536
[7] Martinet E, Reinhardt F, Gustafsson A, Biasiol G and Kapon E 1998 *Appl. Phys. Lett.* **72** 701
[8] Biasiol G, Kapon E, Ducommun Y and Gustafsson A 1998 *Phys. Rev.* B **57** R9416
[9] Biasiol G and Kapon E 1998 *Phys. Rev. Lett.* **81** 2962
[10] Vouilloz F, Oberli D Y, Dupertuis M A, Gustafsson A, Reinhardt F and Kapon E 1997 *Phys. Rev. Lett.* **78** 1580
Vouilloz F, Oberli D Y, Dupertuis M A, Gustafsson A, Reinhardt F and Kapon E 1998 *Phys. Rev.* B **57** 12 378
[11] Akiyama H, Someya T, Yoshita M, Sasaki T and Sakaki H 1998 *Phys. Rev.* B **57** 3765
[12] Arakawa T, Kato Y, Sogawa F and Arakawa Y 1997 *Appl. Phys. Lett.* **70** 646
[13] Lomascolo M, Ciccarese P, Cingolani R, Rinaldi R and Reinhart F K 1998 *J. Appl. Phys.* **83** 302
[14] Kaufman D, Berk Y, Dwir B, Rudra A, Palevski A and Kapon E 1999 *Phys. Rev.* B **59** R10 433
[15] Citrin D S and Chang Y C 1993 *IEEE J. Quantum Electron.* **29** 97
[16] Rossi F, Goldoni G and Molinari E 1997 *Phys. Rev. Lett.* **78** 3527
[17] Ammann C, Dupertuis M A, Bockelmann U and Deveaud B 1997 *Phys. Rev.* B **55** 2420
[18] Chang K and Xia J B 1998 *Phys. Rev.* B **58** 2031
[19] Sun H 1998 *Phys. Rev.* B **58** 15 381
[20] Deng Z Y, Sun H and Gu S W 1992 *J. Phys.: Condens. Matter* **4** 6549
[21] Deng Z Y, Zhang Y F and Guo J K 1995 *J. Phys.: Condens. Matter* **7** 6483
[22] Deng Z Y, Chen X S, Ohji T and Kobayashi T *Phys. Rev.* B at press
[23] Mailhiot C, Chang Y C and McGill T C 1982 *Phys. Rev.* B **26** 4449
[24] Kalt H 1996 *Optical Properties of III–V Semiconductors* (Berlin: Springer) p 177
[25] Bryant G W 1984 *Phys. Rev.* B **29** 6632
Bryant G W 1985 *Phys. Rev.* B **31** 7812
[26] Brown J W and Spector H N 1986 *J. Appl. Phys.* **59** 1179
[27] Deng Z Y, Sun H and Gu S W 1993 *J. Phys.: Condens. Matter* **5** 757

[28] Deng Z Y and Gu S W 1993 *J. Phys.: Condens. Matter* **5** 2261
[29] Weber G, Schulz P A and Oliveira L E 1993 *Phys. Rev.* B **38** 2179
[30] Branis S V, Li G and Bajaj K K 1993 *Phys. Rev.* B **47** 1316
[31] Deng Z Y, Lai T R, Guo J K and Gu S W 1994 *J. Appl. Phys.* **75** 7389
[32] Cao H T and Thoai D B T 1995 *Physica* B **205** 273
[33] Montes A, Duque C A and Porras-Montenegro N 1998 *J. Phys.: Condens. Matter* **10** 5351
[34] Deng Z Y, Guo J K and Lai T R 1994 *Phys. Rev.* B **50** 5736